Pharm Res (2014) 31:2140–2151
DOI 10.1007/s11095-014-1314-6

RESEARCH PAPER

Evaluation of Coating Properties of Enteric-Coated Tablets Using Terahertz Pulsed Imaging

Masahiro Niwa • Yasuhiro Hiraishi • Katsuhide Terada

Received: 14 October 2013 / Accepted: 23 January 2014 / Published online: 27 February 2014

ABSTRACT

Purpose Enteric coatings are used to reduce gastrointestinal side effects and control the release properties of oral medications. Although widely used, the effect of formulation and process conditions on physicochemical and functional properties of enteric coatings remains unclear.

Methods Terahertz pulsed imaging (TPI) was employed to evaluate the coat properties of enteric coated tablets (ECTs) with various acid resistance. Other analytic methods, such as loss on drying, scanning electron microscopy and X-ray computed tomography were then used to validate the relationships established among 4 TPI-derived parameters and the physicochemical properties of enteric coatings.

Results Weight gain measurement did not provide any information to assess acid resistance of enteric coating, whereas four TPI-derived parameters non-destructively reflected the coating properties such as thickness, coat uniformity, density, and water distribution, allowing the identification of the causes of poor acid resistance in certain ECT batches using a single measurement. These parameters also revealed the effect of coating conditions; in particular, coating under dry conditions led to less dense and nonuniform coatings with poor acid resistance.

Conclusion We demonstrated the utility of TPI to identify structural defects within ECTs with poor acid resistance. TPI-derived parameters can aid in formulation development and quality control of ECTs.

M. Niwa (✉) · Y. Hiraishi
Pharmaceutical Technology R&D Laboratories; CMC Center
Takeda Pharmaceutical Company Ltd.
2-17-85 Jusohonmachi, Yodogawa-ku, Osaka 532-8686, Japan
e-mail: masahiro.niwa@takeda.com

K. Terada (✉)
Faculty of Pharmaceutical Sciences, Toho University, 2-2-1 Miyama
Funabashi, Chiba 274-8510, Japan
e-mail: terada@phar.toho-u.ac.jp

KEY WORDS acid uptake · coating uniformity · enteric coated tablets · terahertz pulsed imaging · X-ray CT scan

ABBREVIATIONS

ANOVA	Analysis of variance
API	Active pharmaceutical ingredient
ECT	Enteric coated tablet
LOD	Loss on drying
MFT	Minimum film forming temperature
NIR	Near infrared spectroscopy
SEM	Scanning electron microscopy
TEFPS	Terahertz electric field peak strength
TPI	Terahertz pulsed imaging
XRCT	X-ray computed tomography

INTRODUCTION

Film coatings on medicinal tablets can improve the efficacy, tolerability, and side effect profile of active pharmaceutical ingredients (APIs). For example, coatings can improve chemical stability under high humidity or light exposure, mask unfavorable taste, and control the dissolution profile to obtain the desired plasma concentrations required for therapeutic purposes (1).

One ubiquitous functional coating is enteric coating, which is designed to protect APIs from the acidic environment of the stomach, thereby allowing the release of the drug at the higher pH environment of the upper intestine (2,3). In addition, enteric coatings can obviate side effects such as nausea or bleeding by protecting the gastric mucosa from the irritating effects of drugs (4) or be used to design delayed release formulations (5). Many commercial products such as Prevacid® (Takeda), Dulcolax® (Boehringer Ingelheim), Voltaren® (Novartis), and Epilim® (Sanofi-aventis) are available with enteric coatings. Despite these benefits, the effects of

different formulation and manufacturing conditions on the functional properties of enteric coatings remains still unclear (6,7), resulting in poor acid resistance or other quality variations across batches. One possible reason for this lack of consistency is that coating process has been controlled most often by weight gain measurements (8), which are not always a good indicator for quality assessment. For example, weight gain measurements provide no information on how the film coating is distributed over the surface of the tablet, and it is known that the density of the film coating can vary among batches that demonstrate the same weight gain (9). Coating properties such as thickness, uniformity, density/porosity, tensile strength, and surface roughness are superior indices for quality control. For these measurements, methods such as scanning electron microscopy (SEM) (10), X-ray computed tomography (XRCT) (11), atomic force microscopy (12), laser-induced breakdown spectroscopy (13), near infrared spectroscopy (NIR) (14), and Raman spectroscopy (15) have been investigated. Although these methods provide valuable information, they often do not possess sufficient sensitivity to assess the properties of film coatings. Optical microscopy techniques such as SEM and XRCT do not always provide quantitative information for precise estimates of coating quality (16). Moreover, some of these techniques are destructive and thus difficult to apply for on-line analysis. Raman spectroscopy and NIR are capable of rapid measurement of coating thickness, but the development of chemometric models is necessary since the absorption is related to the amount of coated material. Plus, slight variations in process conditions can shift the spectral response, causing the model to lose its quantitative prediction power (17,18).

Terahertz pulsed imaging (TPI) was introduced to the pharmaceutical industry during the last decade and has been utilized for pharmaceutical dosage form analysis (19,20). One of greatest advantages of TPI in comparison with other techniques is that terahertz radiation (2 cm^{-1}–120 cm^{-1}) is capable of penetrating approximately 3 mm through typical pharmaceutical components to reveal the internal structure. The applied terahertz pulse is reflected according to refractive index changes within the sample. The refractive index changes at the interface of different chemical components or physical structures, which nondestructively reveals the film coating/core tablet interface. The time delay of the reflection from the interface compared with the surface reflection is used for time-of-flight analysis of the depth of the interface; thus, no chemometric calibration models are required for quantification. Moreover, TPI can reveal physicochemical information, which is not directly accessible by surface imaging techniques or by measurement of bulk properties (21). For instance, TPI has been used for evaluating the coating thickness distribution (9,22), the surface density of pharmaceutical tablets (23,24), and for the quality assessment of the interface between buried structures in multilayered tablets (25).

Despite its great potential as an analytical tool, research on TPI applications for pharmaceutical products has been limited. In particular, few studies have investigated the correlation between TPI-derived parameters and the physicochemical properties of the coating and studied the mechanism by which these parameters can be utilized for actual pharmaceutical development. In the present study, the utility of TPI for the analysis of enteric coated tablets (ECTs) was investigated. We manufactured eight ECT batches under different coating conditions to prepare ECT batches with various acid resistances, which is critical functional property of enteric coated products. Then, we analyzed these batches by TPI to evaluate the effect of coating conditions on the physicochemical properties of the coating and also the relationship between the physicochemical properties of the enteric coating and acid resistance. Four unique TPI-derived parameters, i.e., the coating thickness, coating uniformity, terahertz electric field peak strength (TEFPS), and interface index, were then used to investigate of cause of poor acid resistance. Lastly, these results were confirmed using loss on drying (LOD), SEM, and XRCT.

MATERIALS AND METHODS

Samples

D-Mannitol (Pearlitol 50D, Roquette Co. Ltd., Lestrem, France) and microcrystalline cellulose (PH-101, Asahi Kasei Chemicals Co. Ltd., Tokyo, Japan), which are widely used as diluents in pharmaceutical products, were granulated by fluid-bed granulation using hydroxypropyl cellulose (HPC-L, Nippon Soda, Co. Ltd., Tokyo, Japan) as a binder solution. Granules were blended with sodium starch glycolate (Primojel, DFE Pharm, Goch, Germany) and magnesium stearate (Taihei Chemical Industrial Co. Ltd., Osaka, Japan), and compressed on a tablet press (Correct 19K, Kikusui Seisakusho, Kyoto, Japan) at 7 kN and 30 rpm using a 7-mm diameter bi-convex punch. Core tablets were then coated with coating dispersion containing Eudragit L30D-55 (Evonik Industries AG, Darmstadt, Germany), triethyl citrate (TEC) (Morimura Bros., INC., Tokyo, Japan), talc (Matsumura Sangyo Co. Ltd, Osaka, Japan), titanium dioxide (Freund Corporation, Tokyo, Japan), and ferric oxide (LCW, Saint Ouen L'Aumone, France) using a Hi-coater (HC-LABO, Freund Corporation, Tokyo, Japan).

Eight ECT batches were manufactured under different coating conditions (Table I). To study process parameters, we focused on product temperature, spray air volume, and spray rate, which are important parameters required for controlling the properties of film layers and coating efficiency (12,26). Other factors such as charged amount, pan rotation speed, and inlet air volume were held constant at 300 g,

Table I Manufacturing Conditions Used for Enteric Coating

Batch number	Coating condition	Inlet air temperature (°C)	Spray rate (g/min)	Spray air volume (NL/min)	Product temperature (°C)
1	Control	60	3	50	37 ± 1
2	High temperature	80	3	50	52 ± 1
3	Low temperature	40	3	50	21 ± 1
4	High spray air	60	3	80	37 ± 1
5	Low spray air	60	3	30	37 ± 1
6	Dry	80	1.5	80	52 ± 1
7	Wet	40	4.5	30	21 ± 1
8	Without TEC	60	3	50	37 ± 1

25 rpm, and 50 m^3/min, respectively. The coating amount was 6% weight gain (7.2 mg/cm^2) relative to the core tablet (150 mg). TEC, the critical component dictating proper film formation, was not added to ECT batch 8 to investigate its contribution in film formation. Batch 1, fabricated using intermediate values for temperature, spray air volume, and spray rate, was considered as the "control" condition. The combination of these factors determined whether the coating conditions were "wet" or "dry," with low inlet temperature, high spray rate, and low spray air volume constituting the "wet" condition.

Tablet Properties

The weight of ECT was measured using Pharma Test (PHARMA TEST Apparatebau AG, Hainburg, Germany) (n=10). The water content of sample tablets was measured by the loss on drying method using approximately 1 g of tablet from each batch according to the procedure reported in USP 35 NF 30 <731> using DNF 400 (Yamato-kagaku, Tokyo, Japan) at 105°C for 3 h. The equilibrium relative humidity of samples was measured using Hygrolab2 (ROTRONIC AG, Bassersdorf, Switzerland).

Acid Uptake

Acid protection by the enteric coating was evaluated by disintegration tests in two acidic media according to the procedures described in USP 35 NF 30 <701>. Six tablets of each batch were weighed individually and placed in a disintegration tester (Toyama Sangyo Co. Ltd, Osaka, Japan). After 2 h in either high acidity (compendia acid stage, 0.1 N HCl, pH 1.2) or intermediate acidity (acetate buffer, pH 4.5) at 37 ± 1°C, tablets were removed from the vessel. Excess surface media was removed with a paper towel, and the tablets were reweighed. Acid uptake was calculated according to following equation: Acid uptake (%) = 100 × (Wa − Wb)/Wb, where Wb and Wa are tablet weights before and after testing.

Moisture Conditioning and Moisture Content Measurement of ECTs

To condition tablets to different moisture contents, ECTs from batch 1 were placed in a humidity chamber (SH-2219, ESPEC Corp., Osaka, Japan) at 25°C for 2 weeks under 11%, 22%, 33%, 44%, 57%, 68%, 75%, or 85% RH. Tablets were removed from the chamber at 3, 7, and 14 days and weighed to determine the moisture level. After 14 days in the humidity chamber, the equilibration of water content in ECTs was confirmed and TPI was employed. The moisture level was evaluated as a function of equilibrium relative humidity using a water activity analyzer (HygroLab; Rotronic AG, Bassersdorf, Switzerland). The water content of the samples was determined by weighing samples before and after moisture conditioning with correction for intact tablet weight.

SEM

Sample tablets were cut using a Leica EM RAPID milling system (Leica Mikrosysteme GmbH, Solms, Germany) to obtain successive cross-sectional surfaces. Each exposed surface was then sputter-coated with gold film to reduce charging effects. Images were captured using a scanning electron microscope (JSM-6390LV, JEOL, Tokyo, Japan) operating at a 5-kV acceleration voltage.

XRCT

An X-ray microscope (Nano 3DX, Rigaku Corporation, Tokyo, Japan) was used to nondestructively characterize the internal features of ECTs. The sample was placed on a rotating stage between the X-ray source and a two-dimensional (2D) CCD detector. The X-ray source was operated at 50 kV and 24 mA. The spatial resolution was 4.32 μm/pixel. Image stacks (X–Y planes) were reconstructed using Nano three-dimensional (3D) Calc (Rigaku Corporation, Tokyo, Japan) to produce 3D images where each voxel represents the X-ray absorption at a point within the tablet.

TPI

The TPI Imaga2000 system (TeraView Ltd., Cambridge, UK) was used in this study. The technical configuration, including details of the data acquisition process and the image analysis procedure, has been described previously (27,28). The entire imaging process was completely automated using a 6-axis robotic arm. In the first step, a surface model of the sample was generated by a 670-nm laser gauge scan, and this model was used for the subsequent terahertz scan. Individual points of the terahertz scan were then assembled into a 3D image. The emitted terahertz pulse is reflected to a receiver wherever there is a chemical or physical change in the sample, such as at the film coating/core tablet interface, leading to a change in the refractive index and/or absorption coefficient. The time delay of these reflections compared with the surface reflection is used to calculate the depth of the refraction change by time-of-flight measurement. The X–Y pixel resolution was approximately 200 μm with a Z-axis (depth) resolution of 2 μm for layers greater than 40 μm thick. These measurements were performed on both sides of the ECTs using point-to-point scan mode, thin mode (>1.0 mm in air as depth resolution), and a 150-μm step size. Pulse width of 12 and cut-off frequency of 120 was used for data deconvolution so that low noise and sharp peaks are obtained. The refractive index was set to 1.5, which was determined as experimental value from each eight batches using TPI, and the layer thickness and interface index were calculated. All data were acquired using the TPI Coating Scan software version 1.7.3 (TeraView) and analyzed using the TPIcsView software version 2.3.4 (TeraView).

Statistical Analysis

Data were analyzed by Tukey–Kramer's honestly significant difference (HSD) test or analysis of variance (ANOVA) using the JMP software version 8.0 (SAS Institute Inc., Cary, NC, USA). In all cases, a p-value <0.05 was considered significant.

RESULTS AND DISCUSSION

Tablet Weight and Water Content

We fabricated eight ECT batches using different coating conditions (Table I) to yield tablets of varying acid resistance. First, tablet weight and water content of all eight batches were measured (without equilibrating these batches to different moisture atmospheres). There was no significant difference in the mean tablet weight among batches (ANOVA, $p>0.05$) (Table II), which was as expected since the coating amount was constant. On the other hand, LOD appeared to differ among batches depending on the coating condition (ANOVA, $p<0.01$). The "wet" coating condition due to the combination of lower inlet temperature, higher spray rate, and lower spray air volume increased the tablet water content as indicated by LOD measurements.

Acid Uptake

Acid resistance of all eight ECT batches was evaluated by acid uptake in two acidic media (pH 1.2 and 4.5) over 2 h. Acid uptake of no more than 10% was considered sufficient acid resistance (29). Batches 6 and 8 showed insufficient acid resistance at pH 1.2, whereas batch 7 showed poor acid resistance (17.6%) at pH 4.5 (Table II). Batch 8, fabricated without plasticizer, immediately disintegrated in both media, so their acid uptake could not be measured. The other five batches showed sufficient acid resistance, with <10% acid uptake in both acidic media. However, acid resistance varied among batches, indicating that the coating condition substantially affected the physicochemical properties of the enteric coating layer. These results also suggest that weight gain is not a good indicator of coating quality because all eight batches exhibited the same weight gain. TPI was then employed to reveal the difference in the physicochemical properties of these eight ECT batches.

TPI Parameters

Here we evaluated the coating thickness, coating uniformity, terahertz electric field peak strength (TEFPS), and interface index using TPI. Coating thickness is the layer thickness of the enteric coating, which is calculated using the time delay between the terahertz reflections ($\triangle$t), the speed of light (c), and refractive index of the coating (n) in the equation coating thickness (μm) = $\triangle$tc/2n. Coating uniformity is expressed as the averaged standard deviation of the coating thickness examined for ten tablets in each batch. TEFPS is calculated as TEFPS (%) = Rs/Rm × 100, where Rs is the magnitude of the reflected terahertz pulse from the sample surface and Rm is the amplitude of the reference incident terahertz pulse derived from mirror. The reflected wave depends on surface penetration due to density and scatter due to surface roughness, provided information on the surface roughness/density of the coating layer (Fig. 1) (9). Surface roughness/density is an important factor determining tablet surface appearance and media permeability of the coating layer, and is thus associated with acid resistance. The interface index is a value uniquely derived from the time-domain terahertz waveform, which was calculated as interface index (%) = Ri/Rs × 100. Ri is the amplitude of the reflection between coating and core tablet interface. Ri depends on the magnitude of the change in refractive index at the coating/tablet core interface, which may be indicative of the changes in the physical and chemical properties at the interface.

Table II Summary of the Physicochemical Properties and TPI Results of Eight ECT Batches Manufactured Using Different Coating Conditions

Batch #	Tablet weight (mg)[a]	LOD (%)[b]	Acid uptake (%)[c]		TPI[d]			
			pH 1.2	pH 4.5	Thickness (μm)	Coating uniformity (μm)	TEFPS (%)	Interface index (%)
1	158.9 ± 1.6	1.1 ± 0.0	4.9 ± 0.7	6.2 ± 0.5	55.7 ± 4.4	4.6 ± 1.0	21.7 ± 1.2	8.4 ± 1.2
2	158.0 ± 1.9	0.8 ± 0.1	4.9 ± 1.3	6.4 ± 0.9	57.1 ± 2.3	6.0 ± 1.1	21.9 ± 0.3	6.6 ± 1.0
3	158.8 ± 1.5	1.6 ± 0.1	5.6 ± 0.3	8.9 ± 0.9	52.1 ± 3.4	4.0 ± 1.1	22.3 ± 0.3	9.3 ± 0.8
4	158.8 ± 1.4	0.9 ± 0.0	5.2 ± 0.3	6.5 ± 0.6	62.6 ± 5.4	7.1 ± 1.4	21.8 ± 0.3	6.6 ± 0.6
5	158.3 ± 2.0	1.1 ± 0.1	5.8 ± 0.4	8.2 ± 0.6	49.8 ± 1.4	5.4 ± 1.3	22.0 ± 1.6	9.3 ± 1.2
6	158.9 ± 1.2	1.0 ± 0.0	39.1 ± 19.0	19.8 ± 19.9	70.8 ± 3.4	12.0 ± 1.0	19.7 ± 0.4	5.7 ± 0.5
7	158.5 ± 0.9	1.6 ± 0.1	8.2 ± 5.1	17.6 ± 18.2	50.4 ± 0.9	3.6 ± 0.9	22.2 ± 1.0	10.4 ± 0.9
8	159.7 ± 1.3	1.1 ± 0.1	N.D[e]	N.D[e]	58.1 ± 6.6	5.0 ± 1.3	19.9 ± 0.6	8.6 ± 0.8

[a] Data represent the average ± SD of ten measurements

[b] Data represent the average ± SD of three measurements. Data measured using tablets of approximately 1 g from each batch

[c] Data represent the average ± SD of six measurements

[d] Data represent the average ± SD of ten measurements (totally 20 surfaces from 10 top and bottom surfaces)

[e] Not determined due to complete disintegration within 2 h

Figure 2 is the terahertz time-domain waveform from single pixel of the ECT from batch 1 after signal deconvolution. The waveform exhibits a surface peak at 0 mm time delay (air/coating interface) and a negative peak at 0.05–0.1 mm time delay at the coating/tablet core interface. Signal amplitude of reflected pulse was reduced close to tablet edges due to scattering losses (Fig. 2c), measurement in these areas are potentially unreliable in TPI (28). Therefore, the threshold in TEFPS (15–30) was set to exclude the data close to the edges prior to numerical data analysis. In all parameters, the average of data points of a single tablet surface was calculated, and then the average of ten tablets (totally 20 top and bottom surfaces) was calculated for each batch.

Influence of Water Content on TPI Parameters

A previous report found that terahertz radiation was sensitive to water content, similar to other forms of spectroscopy such as NIR (30). Prior to examining all eight ECT batches by TPI, we investigated whether the differences in water content affected the results of TPI analysis. ECTs from batch 1 were placed in a humidity chamber (25°C, 11%–85% RH) for moisture conditioning to yield tablets with different moisture levels prior to TPI. No significant differences were observed in any of the 4 THz parameters over a water content range of 0.6%–3.0% ($p > 0.05$, HSD test) (Table III). The water content of the eight batches ranged from 0.8 to 1.7% (Table II), which was well within the range of the water dependence test. Thus, we concluded that differences in water content among batches would not affect the results of TPI analysis.

Comparison of ECT Batches Using TPI

TPI was performed on all eight ECT batches to distinguish the physicochemical properties of enteric coating layers formed under different conditions and to identify coating parameters associated with poor acid resistance (observed in

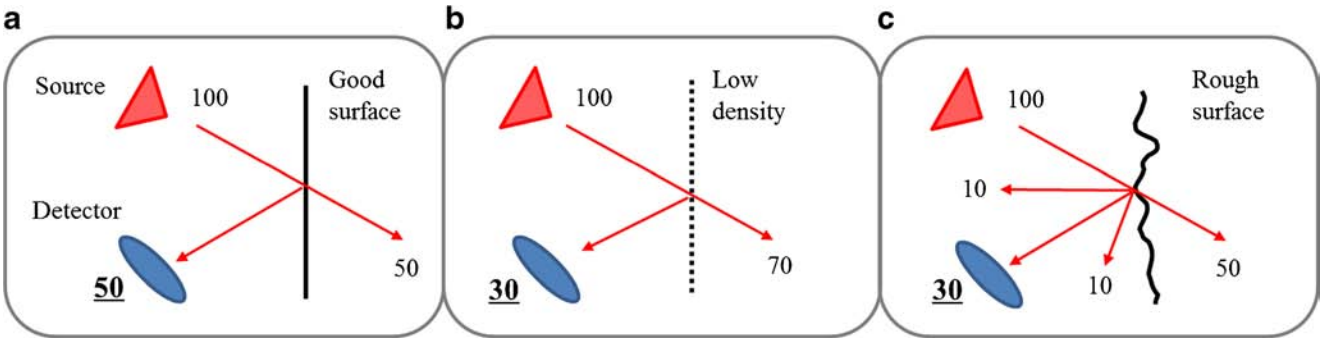

Fig. 1 A schematic of how surface density and roughness of the tablet relates to the magnitude of terahertz electric field peak strength (TEFPS). Lower TEFPS values resulted from penetration of the field into the lower density material (**b**) and scatter by uneven surfaces (**c**).

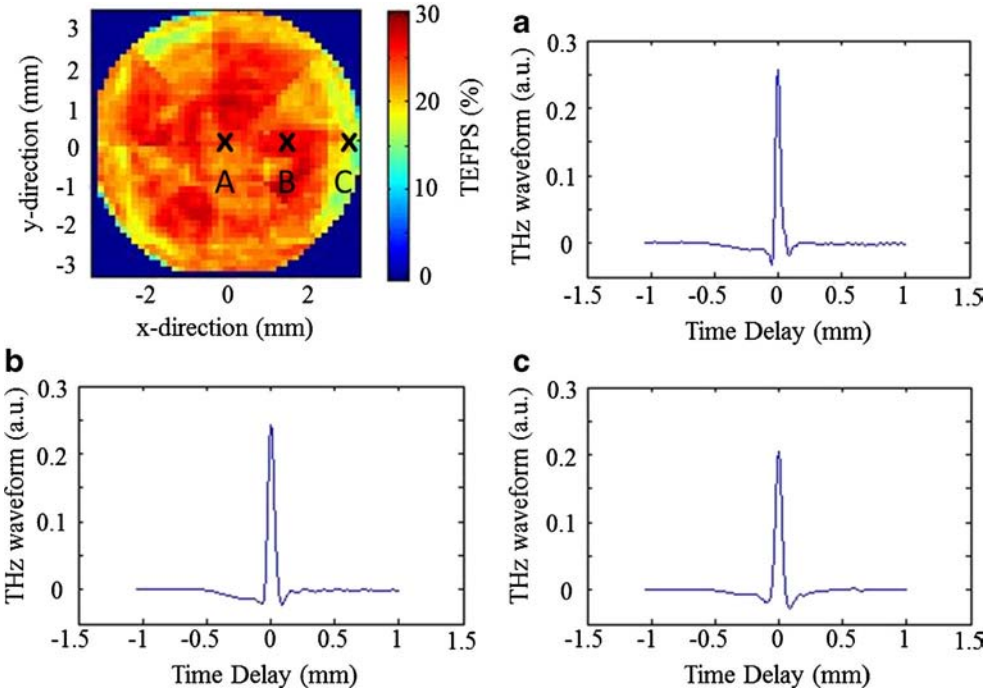

Fig. 2 Terahertz time-domain waveforms of ECT from batch 1 after signal processing (pulse width: 12, cut-off frequency: 120). (**a**) Center, (**b**) middle, and (**c**) close to the edge of the tablet surface, where is marked with x.

samples from batches 6, 7, and 8). These parameters were then compared with weight, LOD, and acid uptake testing results (Table II).

Coating Thickness and Uniformity

Table II shows the coating thickness of each ECT batch measured by TPI. The coating thickness depended on the coating condition (ANOVA, $p<0.01$). Compared with batch 1, the coating tended to become thicker at dry coating conditions (batches 2, 4, and 6), and thinner under wet coating conditions (batches 3, 5, and 7). This may stem from the difference in water content of the atomized polymer droplets delivered to the tablet surface. Water evaporation from the droplets is an important driving force for droplet coalescence required to form a dense coating layer, a certain amount of water is necessary for sufficient coalescence (31,32). Droplets with low water content (under dry coating conditions lose this driving force). Under conditions where the same total amount of coating is deposited, greater thickness implies a less dense coating layer. Batch 8 had similar thickness as batch 1; the presence of TEC had little effect on coating thickness in this study.

Table II shows the coating uniformity of the eight batches. Similar to coating thickness, coating uniformity depended on the coating condition (ANOVA, $p<0.01$). Lower coating uniformity was observed in samples from batches coated under dry coating conditions (batches 2, 4, and 6), whereas greater coating uniformity was observed in samples from batches coated under wet coating conditions (batches 3, 5, and 7).

Table III TPI Results for Batch 1 Samples Stored at Different ERH Conditions

Storage condition	ERH (%)[a]	LOD (%)[a]	Coating thickness (μm)[b]	Coating uniformity (μm)[b]	TEFPS (%)[b]	Interface index (%)[b]
11%	21.9	0.6 ± 0.1	58.5 ± 3.5	4.5 ± 1.3	21.6 ± 0.3	7.7 ± 0.8
22%	26.8	0.9 ± 0.0	58.7 ± 2.5	4.3 ± 0.8	21.6 ± 0.4	7.4 ± 0.9
33%	35.8	1.0 ± 0.0	57.9 ± 0.9	4.2 ± 0.7	21.2 ± 1.1	7.3 ± 0.4
44%	39.6	1.2 ± 0.1	56.4 ± 1.0	4.6 ± 0.7	21.3 ± 1.0	7.5 ± 0.8
57%	45.7	1.5 ± 0.1	59.5 ± 5.7	5.4 ± 1.3	21.0 ± 0.8	7.6 ± 0.7
68%	54.7	1.9 ± 0.0	58.9 ± 4.3	5.6 ± 1.3	21.3 ± 0.5	7.8 ± 0.7
75%	63.5	2.3 ± 0.1	60.7 ± 3.4	5.3 ± 1.6	21.6 ± 0.8	7.9 ± 1.0
85%	75.8	3.0 ± 0.1	57.3 ± 3.8	4.4 ± 1.0	21.8 ± 1.0	8.3 ± 0.7

ERH equilibrium relative humidity, *LOD* loss on drying

[a] Data represent the average ± SD of three measurements. Data measured using tablets of approximately 1 g from each batch

[b] Data represent the average ± SD of ten measurements (totally 20 surfaces from 10 top and bottom surfaces)

Dry coating conditions would cause spray droplets to dry too soon and prevent their spread over the surface of the tablet. Spray drying could also occur in dry condition.

Figures 3 and 4 depicted the 2D and 3D coating thickness distributions of individual sample tablets. Each figure consists of more than 2000 pixels (2D, Fig. 3) or 5,000 pixels (3D, Fig. 4), providing more accurate estimates of acid resistance than optical microscopy. Optical microscopy provides a higher spatial resolution compared with TPI, but it is typically not possible to sample many points as it is largely manual analysis of the interface for thickness estimation (33). The figures show that batch 6 had the thickest coating among eight batches, indicating a more porous, lower density coating compared with batch 1. This high porosity explains the poor acid resistance of batch 6. The 2D images in Fig. 3 also demonstrate the greatly reduced uniformity of the coating thickness in samples from batch 6. Indeed, the thickness distribution is bimodal, with a thicker coating at the center of the tablet face and a thinner coating at the edges of the tablet surface (Fig. 3f). Bi-convex tablets are not geometrically spherical, resulting in variations in the coating uniformity as they pass through the spray zone during coating. The mechanical shear stress on the tablet surface due to inter-tablet rubbing allows smoothing of the film coating (34), but spray droplets may not efficiently spread around by the mechanical shear stress due to low water content under the dry coating conditions used for batch 6. Furthermore, the coating thickness around the periphery (the central band on the side view) was 49.5 ± 2.0 μm (batch 1), 55.4 ± 2.8 μm (batch 6), and 47.8 ± 1.2 μm (batch 7), usually 10%–20% thinner than that in the central tablet top or bottom surfaces (Fig. 4). Although most quality control measures focus on the coating thickness on the tablet surface, the possible thinning of the coating at the periphery would limit acid resistance even if the coating thickness at the central face was acceptable. Thus, the coating thickness around the periphery of the tablet should be assessed more carefully.

To validate the results of coating thickness obtained by TPI, XRCT was employed on samples from batches 1, 6, and 7. Although measurements of coating thickness slightly

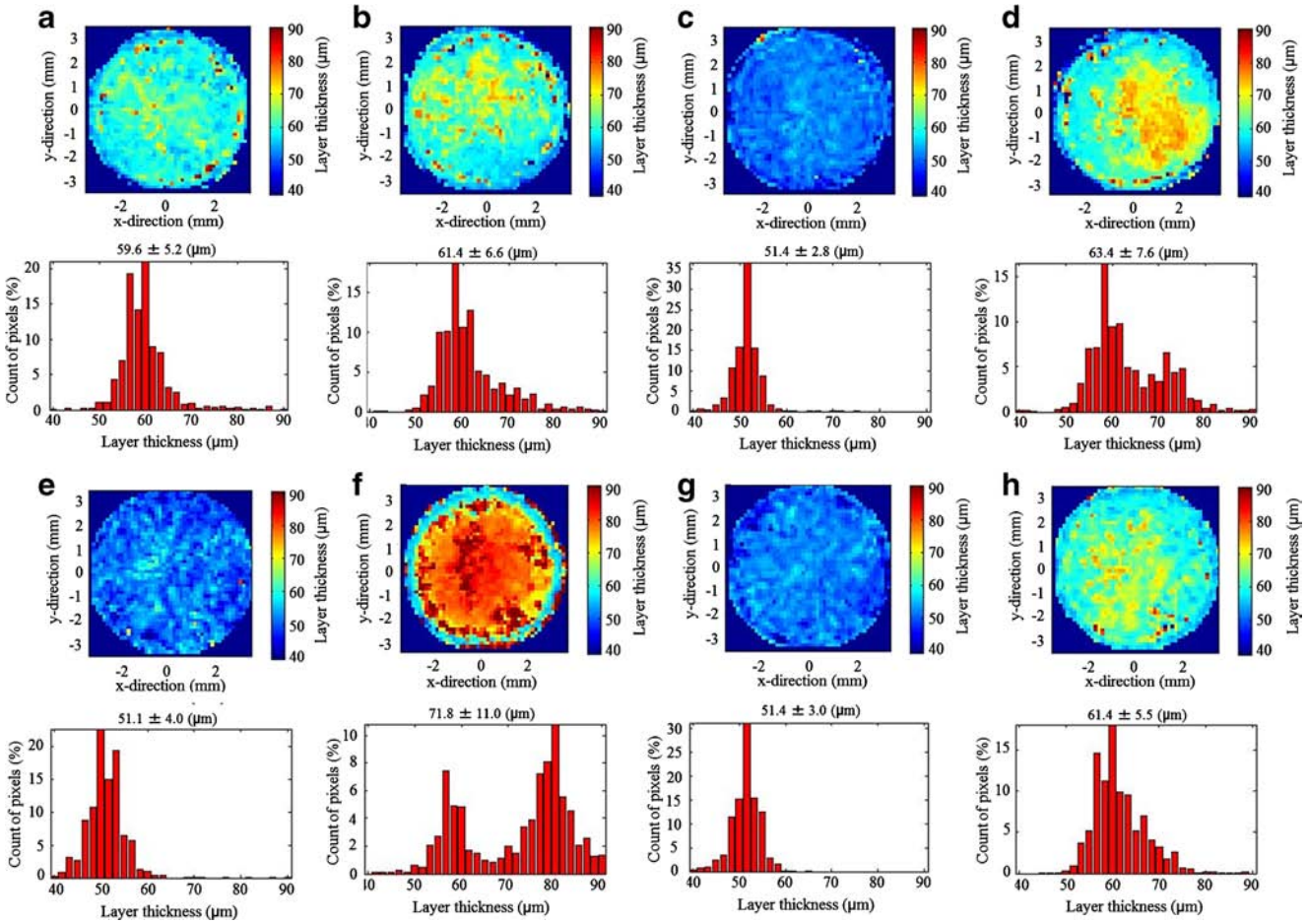

Fig. 3 Two-dimensional coating thickness maps of the ECT surface manufactured at different coating conditions. (**a**) Batch 1 (control), (**b**) batch 2 (high temperature), (**c**) batch 3 (low temperature), (**d**) batch 4 (high spray air), (**e**) batch 5 (low spray air), (**f**) batch 6 (dry), (**g**) batch 7 (wet), and (**h**) batch 8 (without TEC). The figure shows that batch 6 has a thicker and less uniform coating layer than the other batches. In addition, bimodal coating thickness distribution was revealed, and the area near the edge of tablet was found to be thinner than that of the center area.

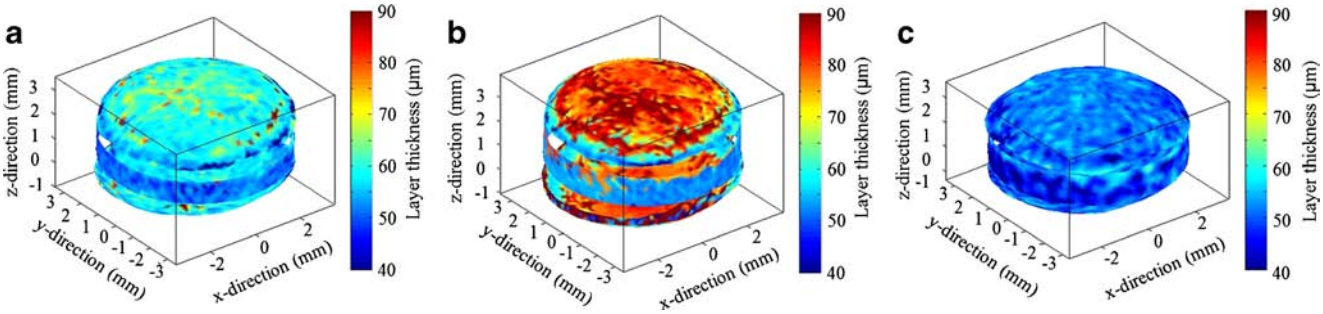

Fig. 4 Three-dimensional coating thickness maps of ECTs manufactured at different coating conditions. The figures consist of three parts, both sides of the tablet surface and a central band. (**a**) Batch 1 (control), (**b**) batch 6 (dry), and (**c**) batch 7 (wet). The figure shows that batch 6 has a thicker coating layer than batch 1, whereas batch 7 has a thinner coating layer than batch 1. In addition, coating thickness around the central band was found to be 10%–20% thinner than that on the tablet surfaces.

differed between methods (Fig. 5), the same trends were apparent in batch coating thickness and uniformity. Differences in absolute thickness estimates between these techniques may arise from the number of sampling points used to calculate the mean (9). For TPI, more than 5,000 pixels from the whole tablet were acquired, providing a more reliable estimate of the coat thickness at each point and thus a better measure of uniformity. A second advantage of TPI over XRCT is that automatically identifying the coating/tablet core interface based on the terahertz reflection allows for more accurate and faster coating thickness determination, whereas XRCT requires visual identification of the interface for thickness estimation.

TEFPS

Table II shows that TEFPS also depended on the coating condition (ANOVA, $p<0.01$). The 2D TEFPS maps of individual batches clearly shows that batches 6 and 8 had lower TEFPS values, indicating a rougher surface or lower density coating compared with other batches (Fig. 6).

SEM images of batches 1, 6, 7, and 8 were acquired to confirm that TEFPS is indicative of physicochemical properties of layer. SEM micrographs revealed smooth surface and densely formed layers of tablets from batches 1 and 7, whereas pores and cracks were found in the coating layers of tablets from batches 6 and 8 (Figs. 7 and 8). Thus, the lower TEFPS was indicative of a rougher surface and lower density coating. The difference in TEFPS may also relate to the water content in the coating layer. TEFPS is a function of the relative difference in refractive index at the surface of tablet, higher TEFPS will be observed with increasing water content in coating layer due to higher refractive index of water (2.0). However, no significant differences were observed in any of the 4 THz parameters over a water content range of 0.6%–3.0% ($p>0.05$, HSD test) (Table III). In addition, batch 8 was

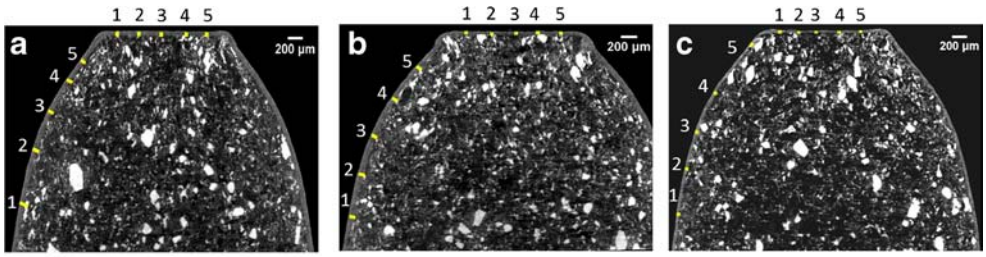

Fig. 5 X-ray computed tomography (XRCT) images of ECTs manufactured at different coating conditions. Each figure is the Y slice at approximately 3.5 mm from the tablet edge. The coating thickness of 5 points from both the surface and the central band were measured using Nano 3D Calc. (**a**) Batch 1 (control) with average coating thicknesses of 61 μm (surface) and 49 μm (central band). (**b**) Batch 6 (dry) with average coating thicknesses of 68 μm (surface) and 48 μm (central band). (**c**) Batch 7 (wet) with average coating thicknesses of 44 μm (surface) and 36 μm (central band).

	a		b		c	
	Top/Bottom (μm)	Central band (μm)	Top/Bottom (μm)	Central band (μm)	Top/Bottom (μm)	Central band (μm)
1	65	48	87	52	41	35
2	61	52	76	43	51	43
3	56	48	65	43	42	30
4	54	43	55	48	52	30
5	69	56	57	52	35	43
Ave.	61	49	68	48	44	36
Std.	6	5	13	5	7	7

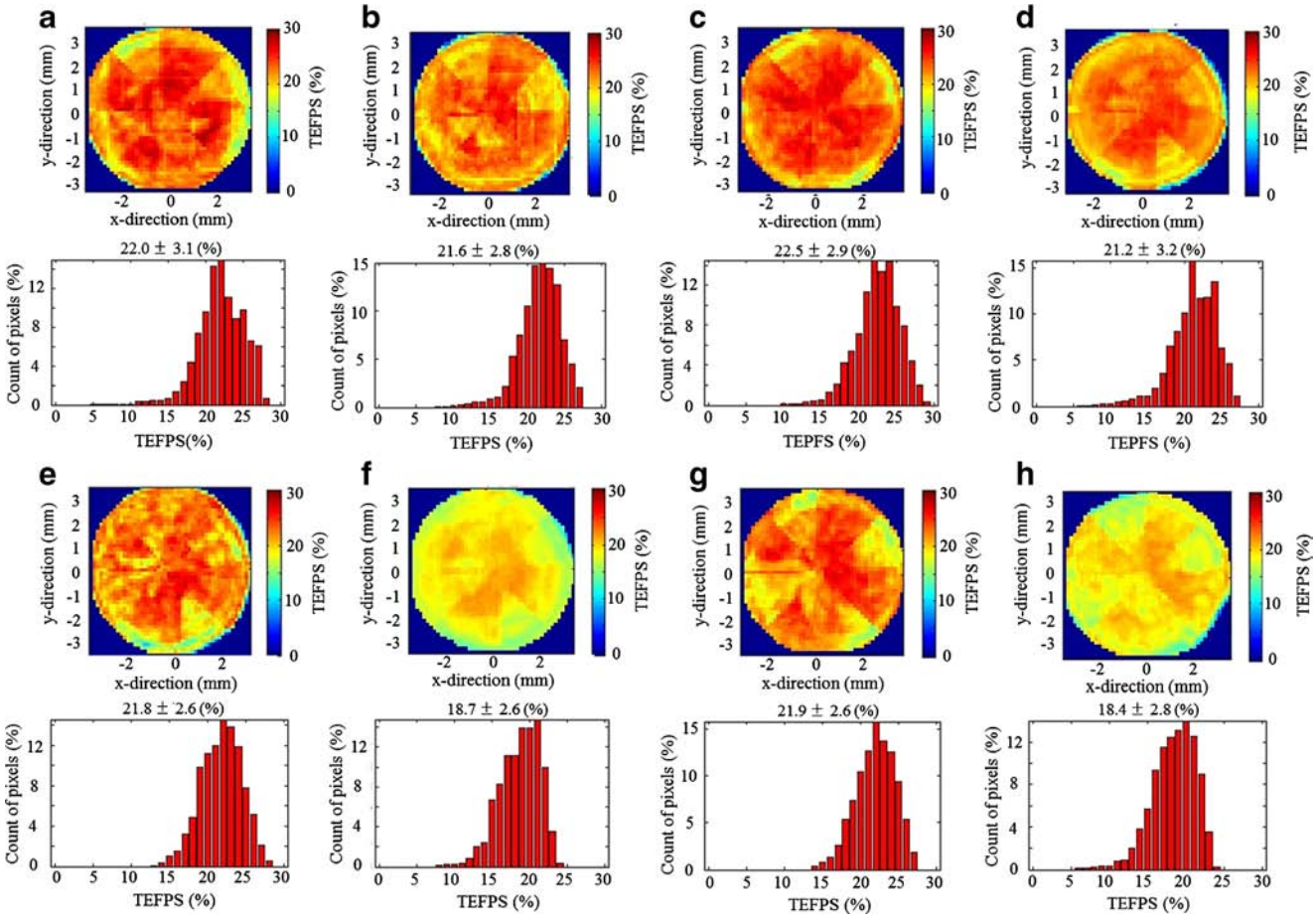

Fig. 6 Two-dimensional terahertz electric field peak strength (TEFPS) maps of the ECT surface manufactured at different coating conditions. (**a**) Batch 1 (control), (**b**) batch 2 (high temperature), (**c**) batch 3 (low temperature), (**d**) batch 4 (high spray air), (**e**) batch 5 (low spray air), (**f**) batch 6 (dry), (**g**) batch 7 (wet), and (**h**) batch 8 (without TEC). The figure shows that batches 6 and 8 had lower TEFPS values, indicating a rougher surface or lower density coating compared with other batches.

the same water content as batch 1 but significantly lower TEFPS. These results suggested that coating density had higher impact on TEFPS rather than water content in the coating layer.

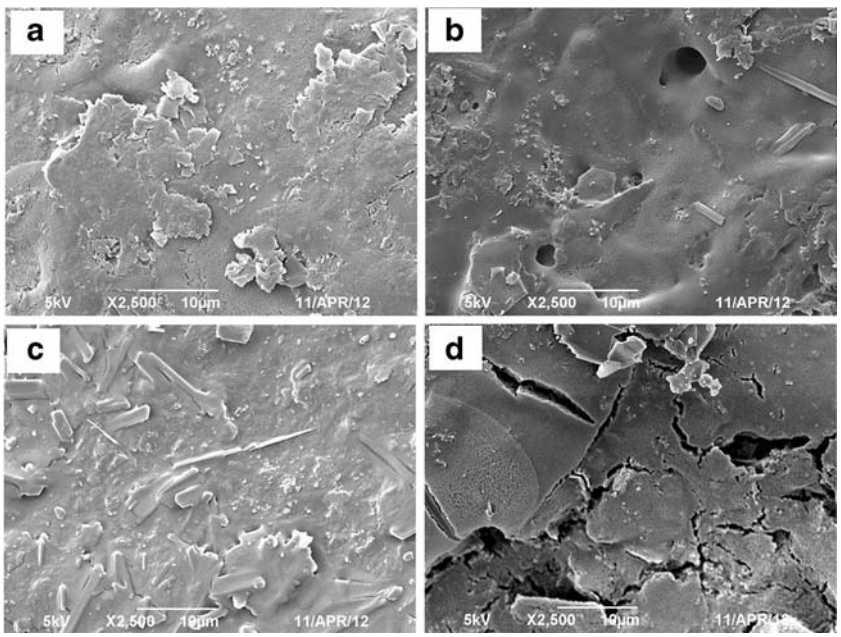

Fig. 7 Scanning electron microscopy (SEM) images of the ECT surface manufactured at different coating conditions. (**a**) No pores or cracks were found in samples from batch 1 (control). (**b**) Many pores were found in samples from batch 6 (dry). (**c**) No pores or cracks were found in samples from batch 7 (wet). (**d**) Many cracks were found in samples from batch 8 (without TEC).

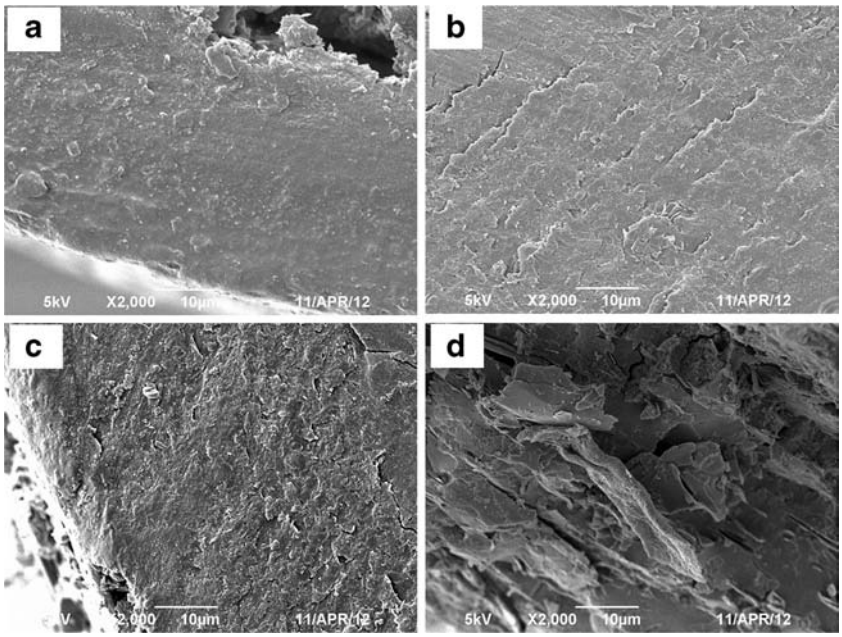

Fig. 8 Scanning electron microscopy (SEM) images of the ECT cross-section manufactured at different coating conditions. Each tablet was cut using a Leica EM RAPID milling system. (**a**) No visual defect was observed in samples from batch 1 (control). (**b**) Cracks were observed in samples from batch 6 (dry). (**c**) No crack or pore, but a slightly different structure in comparison to batch 1, was observed. (**d**) Many cracks were found in samples from batch 8 (without TEC).

These results are also consistent with acid resistance measurements (Table II) as pores and cracks may act as channels for penetration of the acidic medium into the tablet core, resulting in poor acid resistance as observed in samples from batch 6. The porous structure in samples from batch 6 was due to the dry coating condition, which would make spray droplets more similar to dried powder, preventing coalescence and resulting in a porous structure (35). Batch 7 also showed insufficient acid resistance but no obvious structural defects were identified by SEM. We suggest that this "over wet" condition may interrupt water evaporation essential for droplet coalescence (32). In addition, the production temperature during coating (approximately 20°C) in samples from batch 7 may have been too low. The minimum film forming temperature (MFT) of Eudragit L30D-55 containing 10% TEC is approximately 0°C, and a production temperature of at least 10°C–20°C above the MFT is recommended for the coating process. Obara and McGinity (1995) also reported that production temperatures 10°C–15°C above MFT were not always sufficient for aqueous latex dispersion to form a continuous coating layer. The structural defects in samples from batch 8 could be due to lack of plasticizer in the formulation. Plasticizer lowers the MFT of aqueous dispersion and the glass transition temperature of the component polymer by increasing polymer mobility (10), which is essential to avoid film cracking caused by mechanical stress during the coating process or tablet stretching during storage.

Interface Index

The interface index, a measure of the change in refractive index at the boundary between the coating and tablet core, also depended on the coating condition (ANOVA, $p<0.01$) (Table II). The interface index was lower under dry coating conditions (batches 2, 4, and 6), and higher under wet coating conditions (batches 3, 5, and 7). Thus, the interface index may change with the water content within the coating layer. Indeed, the refractive index of the coating layer should increase with increasing water content within coating layer due to the higher refractive index of water (2.0) compared with that of the typical coating components mixture (1.5). Moreover, there was a positive correlation between the interface index and LOD (ANOVA, $p<0.01$, $r=0.723$), further supporting the dependence of the interface index on the coating water content. However, no significant differences in the interface index were observed among batch 1 ECTs equilibrated to different humidity conditions (Table III) even though the water content varied from 0.6 to 3.0%. This could be due to the differences in the water distribution within tablets. In the case of film coating, sprayed water appears to remain within the coating layer, but equilibrating the moisture level in humidity chamber would uniformly hydrate the whole tablet, resulting in the same water content in both film coating and tablet core.

This finding indicates that TPI may allow us to evaluate the water distribution within the tablet, which is difficult by LOD measurements or microscopy. SEM and XRCT could not identify any differences in water content or distribution among batches (Figs. 5 and 8). Although other factors such as density of the coating layer may also affect the interface index (36,37), this contribution appeared limited as batch 8 showed significantly lower density of the coating than batch 1 but had an almost identical interface index value.

Although acid resistance did not depend on the interface index, the main focus of this study, the water content of the

film coating will also greatly affect the quality of the product. For instance, the dissolution profile of sustained release formulations may change depending on the water content in the film coating because water acts as a plasticizer to enhance the coalescence of latex polymers during coating or curing (38). In addition, tablets with water sensitive APIs will become unstable if the coating water content is too high. In these cases, the interface index can be a good indicator for quality control.

Outlook

The present study indicates that TPI can be employed to evaluate the critical properties of enteric coatings, including acid resistance. The four TPI-derived parameters reflect the important physicochemical properties of enteric coatings, allowing for nondestructive identification of structural defect within ECTs. Thus, these parameters may be better indicators for ECT quality control than traditional weight gain measurements. TPI may also reveal how each excipient in the formulation or each operation condition affects the physicochemical properties of the film coating. Many possible quality defects can arise in functional coatings depending on the manufacturing conditions used. Some conditions lead to poor coating uniformity, whereas others may result in a low density coating. Therefore, we have to assess various characteristics of film coatings to accurately predict potential problems and improve formulation/processes. The rich information content of TPI allows for the quantitative evaluation of multiple physicochemical coating film properties, including thickness, uniformity, porosity/density, and water distribution, using a single measurement without destruction of the tablet. Furthermore, nondestructive and calibration-free direct TPI measurements can be used for real-time monitoring of the coating process. A THz sensor for real-time monitoring of coating thickness is currently under development (17).

There are few limitations with the use of TPI. For example, TPI has lower spatial resolution than SEM or XRCT because of the longer wavelength range; hence, it is possible to miss small pores or cracks that could contribute to insufficient acid resistance. The data acquisition to produce imaging data of an entire tablet took about 30 min–60 min depending on measurement conditions, data acquisition speed need to improve for real-time monitoring of film coating process. In addition, the effects of only a few coating process parameters were assessed in this study, whereas many other parameters are known to alter the properties of film coating. Thus, further study is required to extend the range of indices measured by TPI and to validate these against other measurement techniques.

CONCLUSION

In this study, we demonstrated the utility of TPI to investigate the cause of insufficient acid resistance in enteric coatings. Four TPI-derived parameters can nondestructively identify the structural defects within ECTs with poor acid resistance, suggesting that these parameters can be utilized as better indicators for quality control. TPI provides a better understanding of the relationship between formulation/process condition and the resultant properties of enteric coatings, allowing more robust quality control for the development and production of ECTs.

ACKNOWLEDGMENTS AND DISCLOSURES

The authors would like to acknowledge the help of Muneo Nonomura and Ayako Baba in Takeda, Tsuyoshi Miura from Bruker Optics, Jesse Alton and Philip F Taday from Teraview for their valuable suggestions and assistance with this study, which has been a great aid toward the publication of this paper.

REFERENCES

1. Felton LA, Porter SC. An update on pharmaceutical film coating for drug delivery. Expert Opin Drug Deliv. 2013;10:421–35.
2. Missaghi S, Young C, Fegely K, Rajabi-Siahboomi AR. Delayed release film coating applications on oral solid dosage forms of proton pump inhibitors: case studies. Drug Dev Ind Pharm. 2010;36(2):180–9.
3. Fock K, Ang T, Bee L, Lee E. Proton pump inhibitors. Clin Pharmacokinet. 2008;47(1):1–6.
4. Maghsoodi M. Physicomechanical properties of naproxen-loaded microparticles prepared from Eudragit l100. AAPS PharmSciTech. 2009;10(1):120–8.
5. Emerson CR, Marzella N. Dexlansoprazole: a proton pump inhibitor with a dual delayed-release system. Clin Ther. 2010;32(9):1578–96.
6. Felton LA, Porter SC. Guest editor's comments. Drug Dev Ind Pharm. 2010;36(2):127.
7. Suzzi D, Radl S, Khinast JG. Local analysis of the tablet coating process: impact of operation conditions on film quality. Chem Eng Sci. 2010;65(21):5699–715.
8. Ho L, Müller R, Römer M, Gordon KC, Heinämäki J, Kleinebudde P, *et al.* Analysis of sustained-release tablet film coats using terahertz pulsed imaging. J Control Release. 2007;119(3):253–61.
9. Ho L, Müller R, Gordon KC, Kleinebudde P, Pepper M, Rades T, *et al.* Applications of terahertz pulsed imaging to sustained-release tablet film coating quality assessment and dissolution performance. J Control Release. 2008;127(1):79–87.
10. Thoma K, Bechtold K. Influence of aqueous coatings on the stability of enteric coated pellets and tablets. Eur J Pharm Biopharm. 1999;47(1):39–50.
11. Perfetti G, Van de Casteele E, Rieger B, Wildeboer WJ, Meesters GMH. X-ray micro tomography and image analysis as complementary methods for morphological characterization and coating thickness measurement of coated particles. Adv Powder Technol. 2010;21(6):663–75.
12. Perfetti G, Alphazan T, van Hee P, Wildeboer WJ, Meesters GMH. Relation between surface roughness of free films and process parameters in spray coating. Eur J Pharm Sci. 2011;42(3):262–72.
13. Madamba MC, Mullett W, Debnath S, Kwong E. Characterization of tablet film coatings using a laser-induced breakdown spectroscopic technique. AAPS PharmSciTech. 2007;8(4):184–90.

14. Kirsch J, Drennen J. Near-infrared spectroscopic monitoring of the film coating process. Pharm Res. 1996;13(2):234–7.
15. Hagrasy A, Chang S-Y, Desai D, Kiang S. Raman spectroscopy for the determination of coating uniformity of tablets: assessment of product quality and coating pan mixing efficiency during scale-up. J Pharm Innov. 2006;1(1):37–42.
16. Seitavuopio P, Rantanen J, Yliruusi J. Tablet surface characterisation by various imaging techniques. Int J Pharm. 2003;254(2):281–6.
17. May RK, Evans MJ, Zhong S, Warr I, Gladden LF, Shen Y, *et al.* Terahertz in-line sensor for direct coating thickness measurement of individual tablets during film coating in real-time. J Pharm Sci. 2011;100(4):1535–44.
18. Momose W, Yoshino H, Katakawa Y, Yamashita K, Imai K, Sako K, *et al.* Applying terahertz technology for nondestructive detection of crack initiation in a film-coated layer on a swelling tablet. Results Pharma Sci. 2012;2:29–37.
19. Shen Y-C. Terahertz pulsed spectroscopy and imaging for pharmaceutical applications: a review. Int J Pharm. 2011;417(1–2):48–60.
20. Zeitler JA, Taday PF, Newnham DA, Pepper M, Gordon KC, Rades T. Terahertz pulsed spectroscopy and imaging in the pharmaceutical setting—a review. J Pharm Pharmacol. 2007;59(2):209–23.
21. Zeitler JA, Gladden LF. In-vitro tomography and non-destructive imaging at depth of pharmaceutical solid dosage forms. Eur J Pharm Biopharm. 2009;71(1):2–22.
22. Spencer JA, Gao Z, Moore T, Buhse LF, Taday PF, Newnham DA, *et al.* Delayed release tablet dissolution related to coating thickness by terahertz pulsed image mapping. J Pharm Sci. 2008;97(4):1543–50.
23. May RK, Su K, Han L, Zhong S, Elliott JA, Gladden LF, *et al.* Hardness and density distributions of pharmaceutical tablets measured by terahertz pulsed imaging. J Pharm Sci. 2013;102(7):2179–86.
24. Niwa M, Hiraishi Y. Quantitative analysis of visible surface defect risk in tablets during film coating using terahertz pulsed imaging. Int J Pharm. 2014;461(1–2):342–50.
25. Niwa M, Hiraishi Y, Iwasaki N, Terada K. Quantitative analysis of the layer separation risk in bilayer tablets using terahertz pulsed imaging. Int J Pharm. 2013;452(1–2):249–56.
26. Wang J, Hemenway J, Chen W, Desai D, Early W, Paruchuri S, *et al.* An evaluation of process parameters to improve coating efficiency of an active tablet film-coating process. Int J Pharm. 2012;427(2):163–9.
27. Shen YC, Taday PF. Development and application of terahertz pulsed imaging for nondestructive inspection of pharmaceutical tablet. IEEE J Sel Top Quantum Electron. 2008;14:407–15.
28. Brock D, Zeitler JA, Funke A, Knop K, Kleinebudde P. Critical factors in the measurement of tablet film coatings using terahertz pulsed imaging. J Pharm Sci. 2013;102(6):1813–24.
29. Liu F, Merchant HA, Kulkarni RP, Alkademi M, Basit AW. Evolution of a physiological pH6.8 bicarbonate buffer system: application to the dissolution testing of enteric coated products. Eur J Pharm Biopharm. 2011;78(1):151–7.
30. Jördens C, Wietzke S, Scheller M, Koch M. Investigation of the water absorption in polyamide and wood plastic composite by terahertz time-domain spectroscopy. Polym Test. 2010;29(2):209–15.
31. Ludwig I, Schabel W, Ferlin P, Castaing JC, Kind M. Drying, film formation and open time of aqueous polymer dispersions. Eur Phys J Spec Top. 2009;166(1):39–43.
32. Obara S, McGinity JW. Influence of processing variables on the properties of free films prepared from aqueous polymeric dispersions by a spray technique. Int J Pharm. 1995;126(1–2):1–10.
33. Brock D, Zeitler JA, Funke A, Knop K, Kleinebudde P. A comparison of quality control methods for active coating processes. Int J Pharm. 2012;439(1–2):289–95.
34. Ho L, Müller R, Krüger C, Gordon KC, Kleinebudde P, Pepper M, *et al.* Investigating dissolution performance critical areas on coated tablets: a case study using terahertz pulsed imaging. J Pharm Sci. 2010;99(1):392–402.
35. Roy A, Ghosh A, Datta S, Das S, Mohanraj P, Deb J, *et al.* Effects of plasticizers and surfactants on the film forming properties of hydroxypropyl methylcellulose for the coating of diclofenac sodium tablets. Saudi Pharm J. 2009;17(3):233–41.
36. Zeitler JA, Shen Y, Baker C, Taday PF, Pepper M, Rades T. Analysis of coating structures and interfaces in solid oral dosage forms by three dimensional terahertz pulsed imaging. J Pharm Sci. 2007;96(2):330–40.
37. Ervasti T, Silfsten P, Ketolainen J, Peiponen K-E. A study on the resolution of a terahertz spectrometer for the assessment of the porosity of pharmaceutical tablets. Appl Spectrosc. 2012;66(3):319–23.
38. Yang QW, Flament MP, Siepmann F, Busignies V, Leclerc B, Herry C, *et al.* Curing of aqueous polymeric film coatings: importance of the coating level and type of plasticizer. Eur J Pharm Biopharm. 2010;74(2):362–70.